Available online at www.sciencedirect.com
ScienceDirect
Acta Biomaterialia 3 (2007) 209–220
Acta BIOMATERIALIA
www.actamat-journals.com

The influence of sterilization processes on the micromechanical properties of carbon fiber-reinforced PEEK composites for bone implant applications

A. Godara [a], D. Raabe [a,*], S. Green [b]

[a] *Max-Planck-Institut für Eisenforschung, Max-Planck-Str. 1, 40237 Düsseldorf, Germany*
[b] *Invibio Ltd., Hillhouse International Thornton, Cleveleys, Lancashire FY5 4QD, UK*

Received 18 August 2006; received in revised form 26 October 2006; accepted 22 November 2006

Abstract

The effect of sterilization on the structural integrity of the thermoplastic matrix composite polyetheretherketone (PEEK) reinforced with carbon fibers (CF) is investigated by nanoindentation and nanoscratch tests. The use of the material as a medical implant grade requires a detailed understanding of the micromechanical properties which primarily define its *in vivo* behavior. Sterilization is a mandatory process for such materials used in medical applications like bone implants. The steam and gamma radiation sterilization processes employed in this study are at sufficient levels to affect the micromechanical properties of some polymer materials, particularly in the interphase region between the polymer matrix and the reinforcing fibers. Nanoindentation and nanoscratch tests are used in this work to reveal local gradients in the hardness and the elastic properties of the interphase regions. Both methods help to explore microscopic changes in the hardness, reduced stiffness and scratch resistance in the interphase region and in the bulk polymer matrix due to the different sterilization processes employed. The results reveal that neither steam nor gamma radiation sterilization entails significant changes of the reduced elastic modulus, hardness or coefficient of friction in the bulk polymer matrix. However, minor material changes of the PEEK matrix were observed in the interphase region. Of the two sterilization methods used, the steam treatment has a more significant influence on these small changes in this region and appears to increase slightly the thickness of the interphase zone.

Keywords: Biomaterial; Composite; PEEK; Carbon fibers; Bone implant

1. Introduction

The macroscopic behavior of composites depends not only on the properties of their individual constituents but also on the elastic–plastic interaction between the different phases, such as fiber and matrix. During processing of a polymer matrix composite material, the interaction between the surfaces of the fibers and the polymer matrix may create various chemical and morphological inhomogeneities. These are typically discussed in terms of two distinct regions, namely, the interface and the interphase zones. The inter*face* is defined at the atomic scale as the layer of the immediate chemical bond between the fiber and the polymer matrix. The inter*phase* region is much larger. It is formed by local changes of the polymer matrix in the vicinity of a fiber. In this region local properties like morphology, thermomechanical behavior and chemical composition can differ from the corresponding values observed in the bulk polymer matrix [1–3]. It is obvious that the overall mechanical properties of fiber-reinforced polymer composite materials are influenced by the micromechanical behavior of both the interface and the interphase regions.

Sterilization is a mandatory process for materials used in medical applications like bone implants. Sterilization procedures commonly employed are steam sterilization

* Corresponding author. Tel.: +49 (0)211 6792340; fax: +49 (0)211 6792333.
E-mail addresses: a.godara@mpie.de (A. Godara), d.raabe@mpie.de (D. Raabe), sgreen@invibio.com (S. Green).

1742-7061/$ - see front matter © 2006 Acta Materialia Inc. Published by Elsevier Ltd. All rights reserved.
doi:10.1016/j.actbio.2006.11.005

and sterilization by radiation, such as gamma radiation. These two methods are employed in the present study at a level sufficient to affect the micromechanical properties of some polymer materials, particularly in the interphase region between the polymer matrix and the reinforcing fibers. The influence of the steam or radiation treatment, respectively, is known to affect the amount of moisture that can be absorbed by the polymer.

The structural integrity and overall performance of fiber-reinforced polymer composites are strongly influenced by the stability of the fiber/polymer interfacial region. The absorption of moisture causes dilatational expansion and induces stresses which are associated with the moisture-induced expansion entailing degradation of the structural stability [4]. The mechanism of moisture absorption in the polymer matrix or at the interface region is by diffusion or capillary processes [5–7]. This may induce plastic deformation by plasticization or differential strains due to swelling while stretching the polymeric chains [8]. These effects may strongly alter the physical, chemical and mechanical characteristics of the material at different scales [9]. This results in a significant mismatch in moisture-induced volumetric expansion between the matrix and the fibers, and thus leads to the evolution of localized stress and strain fields in fibrous composites [10,11]. Mensitieri et al. [12] studied the diffusion kinetics of water from vapors with different activity and from liquid state into amorphous and semicrystalline PEEK sheets at different temperatures, respectively. At higher activity levels, the amorphous material showed the occurrence of a relaxation process. However, the water uptake values obtained for both amorphous and semicrystalline PEEK confirmed the good moisture and liquid water resistance of this kind of high-performance thermoplastic polymer. However, the water absorption behavior can be very different under external stress conditions in terms of both the rate of penetration and the solubility (swelling) processes [13]. In these cases the authors reported an increase in the kinetics associated with both processes.

The effects of radiation are also of considerable scientific and commercial importance to the material investigated. Previous studies [14,15] on ultra-high molecular weight polyethylene (UHMWPE) have shown an influence of gamma radiation at low doses. The authors concluded that irradiation at low doses produces simultaneous cross-linking and chain scission events that occurred preferentially in the amorphous phase and at the crystal fold surfaces. At high doses, they concluded that chain scission may become a significant competitive process to cross-linking [16]. Such chain scission phenomena may lead to an increased crystallinity by cutting molecules that may then join the crystalline regions, thereby increasing crystallinity and T_g. If irradiated specimens are melted and recrystallized, the cross-linking may inhibit crystallization associated with reduced crystallinity, and therefore modify the mechanical properties [15]. Similar low-energy gamma irradiation at low temperature studies on PEEK have shown excellent mechanical properties [17]. The mechanical properties at high temperature were improved by the formation of cross-links and by an increase in the glass transition temperature of the PEEK matrix [17–19].

A main feature of the mechanical behavior of such complex microstructures is the formation of heterogeneous plastic-flow patterns when stressed. When complex composite materials are subjected to external mechanical loads, the lateral distribution of the accumulated residual deformation is heterogeneous, entailing strain localization. Such strain localization phenomena in general may lead to crack initiation via fiber breakage, microvoid formation, or debonding between matrix and fibers. The resistance of the interphase to transverse crack propagation is important in preventing surrounding fibers from experiencing the effects of the stress concentration that could ultimately lead to additional fiber failure.

The mechanical properties of many composites for biomedical applications depend to a large extent on the processing and loading history to which they are exposed before their actual use in the body. One of the most important factors in that context is the influence of the cooling and loading rates on the fiber–matrix interface adhesion [20–23]. The interface adhesion between PEEK and carbon fibers was correlated to the degree of crystallinity and the crystalline morphology, as well as to the bulk mechanical properties of neat PEEK resin, all of which were in turn controlled by the cooling rate [20,21]. It was shown that the interface bond strength, the tensile strength and the elastic modulus of PEEK resin decreased while the ductility became better with increasing cooling rate due to its positive effect on crystallinity and spherulite size. The improvement of crystalline perfection and flattened lamella chains with high crystallinity in the interphase regions were mainly responsible for the strong interface bond in carbon fiber-reinforced PEEK composites processed at a low cooling rate. The interphase failure was characterized by brittle debonding in slow-cooled composites, whereas the amorphous PEEK-rich interphase introduced in fast-cooled specimens failed in a ductile manner with extensive plastic yielding [22,23].

The width of the interphase regions between either phenolic or polyester matrices and the glass fibers embedded in them showed the cumulative influence of the processing history and of the type of experiment [24–26]. It was also observed that the shape of the indenter is important and that scratch tests proved in part to be more reliable for the integral micromechanical characterization of the interphase region then nanoindentation. Gregory et al. [26] made comparative studies between different *in situ* neat polymer matrix materials such as epoxy resin and PEEK. The results revealed that for both types of matrix materials the modulus and the hardness were affected in the same fashion by the manufacturing process. In another work along these lines it was reported that the influence of environmental exposure can alter the micromechanical response of some polymers and induce aging phenomena.

These entail degradation effects that act on the viscoelasticity, stiffness and hardness [27].

Another aspect is that a chemical treatment of fiber surfaces which is referred to as "sizing" can play a significant role in the adhesion between matrix and fibers by interfering with the interpenetrating diffusion process at the interface region and into the interphase region. Such effects were noticed in a glass fiber-reinforced epoxy composite when the glass fiber surfaces were treated with the coupling agent γ-aminopropyltriethoxy silane (γ-APS) in conjunction with polypropylene or polyurethane film formers in an aqueous spinning bath [28]. This treatment led to different thickness values for the interphase region in similar fiber–matrix systems [28]. Based on the analysis of such boundary effects, with the help of nanoindentation studies, Gao et al. [28] showed that an interphase zone with a higher modulus and a transcrystalline microstructure simultaneously increased the tensile strength and the impact toughness of carbon fiber-reinforced PEEK composites. Tai et al. [29] examined the effects of low-energy impact and cyclic thermal loading on the fatigue behavior of carbon fiber-reinforced PEEK laminates. The thermal cycling did not significantly affect the tensile strength of the impacted laminates but broadened the strength distribution. The fatigue tests showed that both the low-energy impact and the cyclic thermal loading properties reduced the fatigue life of carbon fiber-reinforced PEEK composites significantly. The influence of cyclic thermal loading on the fatigue life was more obvious than the low-energy impact. The carbon fiber-reinforced PEEK laminate displayed better fatigue resistance than carbon fiber-reinforced epoxy laminates. X-ray inspections indicated that no cracks were generated due to the cyclic thermal exposure.

The material investigated in the present study is of medical implant grade because of its versatility, mechanical strength and biocompatibility. Medical device manufacturers have routinely used implantable-grade PEEK polymer in long-term medical implant applications. Therefore, the sterilization treatments are of considerable scientific and commercial importance to the material investigated. The concise literature survey on experimental [1–29] observations conducted on fiber-reinforced polymer composites shows that the overall performance of these materials is influenced in particular by the micromechanical properties of the interphase region. Therefore, a detailed understanding of its micromechanical properties, which primarily define the *in vivo* behavior, is required.

The nanoindentation technique is able to detect material properties like hardness and reduced modulus of different constituents in composite systems with high lateral resolution. Hodzic et al. [24,25] employed the combination of nanoindentation, atomic force microscopy and nanoscratch tests to characterize the micromechanical properties of polymer–glass composites with the aim of determining the width of the interphase regions. Their methodology has been adopted for the present study and results are discussed following a similar approach of analysis to compare the influences of the sterilization processes on the mechanical changes, emphasizing the interface/interphase region of PEEK and CF.

2. Experimental methods

2.1. Material

The investigated composite material, consisting of PEEK as the polymer matrix and carbon fibers as the reinforcing fibers, was provided by Invibio Ltd. The material was in accordance with the supply manufacturing definition and supported by a certificate of analysis. The material was prepared by Invibio Ltd. by extrusion compounding, consistent with normal practice in the polymer industry, but under enhanced processing conditions adopted for medical use. The supplied 3K fiber bundles, with a proprietary surface size, were chopped to 6 mm before introducing into a twin screw compound extruder at a feed ratio of 35 wt.% fiber to 65 wt.% PEEK polymer matrix and extruded as laces of 2–3 mm diameter, which subsequently were chopped into pellets 3–4 mm long. The fibers were coated via a chemical process. The test specimens used in this work were injection molded into sheet-shaped forms with dimensions $150 \times 150 \times 4$ mm in accordance with processing guidelines, including pre-drying of the material overnight at 120 °C. After the injection molding process the average residual length of the carbon fibers was confirmed to be between 200 and 250 μm, as determined by a digital image analysis method.

2.2. Specimen surface preparation

The polishing step is crucial for a proper evaluation of the interface properties. A cross-section area (4×10 mm) of the specimens was polished according to the polishing protocol shown in Table 1 by Cloeren Technology, Germany. Careful attention was paid to the alignment of the sample so that the longitudinal, or fiber, direction was perpendicular to the surface to be polished. The specimens

Table 1
Polishing protocol to prepare the surface of the test specimens (Cloeren Technology)

	Grinding (G)	Grinding (G)	Polishing I (F)	Final polishing II (F)
Substrate	SiC paper	SiC paper	PT AlO_x	PT Chem
G/F-material	SiC	SiC	Aluminum oxide	OxyPol
Grain size	600	1200	–	50 nm
Lubricant	Water	Water	–	–
Rotation	300	300	150	150
Force	25 N	25 N	25–30 N	15 N
Time	Until planar surface	1 min	3–5 min	1–2 min

were mounted in a two-part epoxy and cured overnight. In order to obtain the best possible polished surface, the epoxy was mixed extensively until a homogeneous state was achieved. The air bubbles were removed by keeping the mounted sample in a vacuum chamber before curing overnight. Excess epoxy was removed prior to polishing. The polishing procedure involved a series of silicon carbide (SiC) sandpaper from 600 to 1200 grit and a special polishing pad requiring aluminum pastes and suspensions.

2.3. Sterilization treatment

In order to investigate the influence of different sterilization treatments on the micromechanical properties, a test specimen which was not subjected to any sterilization treatment (reference specimen) was compared with the sterilized test specimens. The sterilization methods employed were a set of steam sterilization cycles (steam-treated specimen) and a gamma irradiation treatment (gamma-irradiated specimen). Both procedures were conducted in accordance with the ISO quality management system standards [30]. The steam sterilization process was performed by Münchener Medizin Mechanik, Germany. It involved three steam cycles of about 50 min each. The temperature and pressure of the sterilization chamber during the process were maintained at 134 °C and 3.115 mbar, respectively. The gamma irradiation was performed by Isotron Deutchland, Germany. The samples were irradiated with an affluence of 75 kGy.

2.4. Nanoindentation and nanoscratching

The tests were conducted using a Hysitron nanoindenter system (TriboIndenter). The instrument includes an XYZ-sample-stage and a set-up which combines a piezo-scanner with a transducer and a Berkovich diamond indenter tip. The XYZ-stage is used to position the sample under the piezo-scanner for the fine positioning as well as the approach of the indenter in the normal direction. After positioning the indenter tip on top of the sample, it can be either directed into the sample by applying a bias voltage on the bottom capacitor of the transducer (hardness test) or it can be moved in a lateral direction, i.e. within the x–y plane (scratch test), with the help of a piezo controller. The piezo controller images the sample surface comparable to a conventional atomic force microscope.

The reduced elastic modulus was calculated by the Oliver and Pharr method [31], which is included in the Hysitron software (Triboview version 6.0.0.31). The contact stiffness S, defined as the slope at the beginning of the unloading curve, is given by:

$$S = \frac{\mathrm{d}P}{\mathrm{d}h} \tag{1}$$

where P is the indentation load and h the indentation depth. For the determination of the slope, the initial portion of the unloading curve is fitted by a power law:

$$P = \alpha \times (h - h_{\mathrm{f}})^{m} \tag{2}$$

where α contains geometric constants, the elastic modulus and the Poisson's ratio of both the sample and the indenter, m is power law exponent that is related to the geometry of the indenter, and h_{f} is the final indentation depth. The elastic modulus E of the indented material is related to the contact stiffness by:

$$S = \frac{2\beta}{\sqrt{\pi}} \times \left(\frac{1 - v^2}{E} + \frac{1 - v_{\mathrm{i}}^2}{E_{\mathrm{i}}} \right)^{-1} \times \sqrt{A_{\mathrm{c}}} \tag{3}$$

where v is the Poisson's ratio and E is the elastic modulus of the material, and v_{i} is the Poisson's ratio and E_{i} is the elastic modulus of the indenter material. A_{c} is the contact area of the indenter and β is a constant for the indenter geometry (1.034 for the Berkovich indenter). Consequently, the reduced elastic modulus, E_{red}, can be defined as:

$$E_{\mathrm{red}} = \frac{\sqrt{\pi}}{2\beta} \times \frac{S}{\sqrt{A_{\mathrm{c}}}} \tag{4}$$

It is linked to the elastic modulus E by:

$$E_{\mathrm{red}} = \frac{E}{1 - v^2} \tag{5}$$

if the indenter is considered to be much stiffer than the probed material. The hardness is defined by:

$$H = \frac{P_{\max}}{A_{\mathrm{c}}} \tag{6}$$

where $P_{\max}$ is the maximal achieved loading force.

The coefficient of friction, μ, is determined from the ratio of the lateral force, F_{L}, (tangential force) and the normal force, F_{N}, at the constant applied load of 100 μN. Therefore, the coefficient of friction indicates the resistance of the material to the tip penetration in the tangential direction (Fig. 1).

2.4.1. Nanoindentation test protocol

The nanoindentation tests were conducted in a load-controlled mode with a Berkovich indenter. A triangular

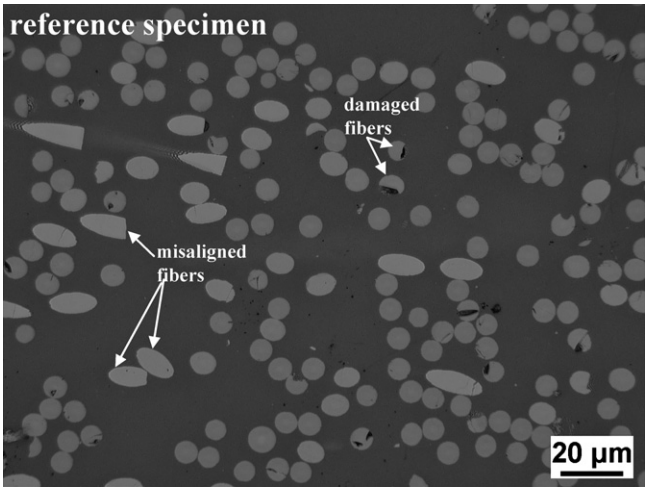

Fig. 1. Optical micrograph of the polished surface of the reference specimen (not subjected to any sterilization treatment) indicating some of the misaligned and damaged fibers.

loading–unloading function with a maximum peak load of 70 μN was applied. The peak load was achieved within 5 s and was removed again in 5 s without any holding time (Fig. 2b). The indent pattern of 1×50 indents (one line of 50 indents) was chosen in such a way that it covered the carbon fiber and the matrix present on both sides of the fiber (Fig. 2a). Simultaneously the displacement of the indenter was measured to give a load–displacement curve. In order to avoid overlapping of the plastic zones created by neighboring indents, the optimal distance between them was evaluated by performing indentation tests at a peak load of 70 μN with different adjacent spacings between the successive indents. Thereafter, the width of the indentation marks was obtained by *in situ* scanning probe microscopy topographic images, Fig. 3. The images were recorded using an *in situ* imaging mode provided by the TriboIndenter (Hysitron). In its *in situ* imaging mode the TriboIndenter utilizes the indenter stylus with a small static force to scan the surface like an atomic force microscope operating in contact mode. As a result, small features in the scan can be addressed with a high positioning accuracy.

In the present study the total width of the plastic zone, indicated by the pile-ups around an indent, was around 0.35 μm. Hence, the successive indents were separated by 0.5 μm. There is no indication of a plastic zone overlapping at the applied peak load. The experiments were repeated several times for each specimen at several positions of similar matrix/fiber arrangements. For the calculation of both the elastic modulus and the hardness from the load–

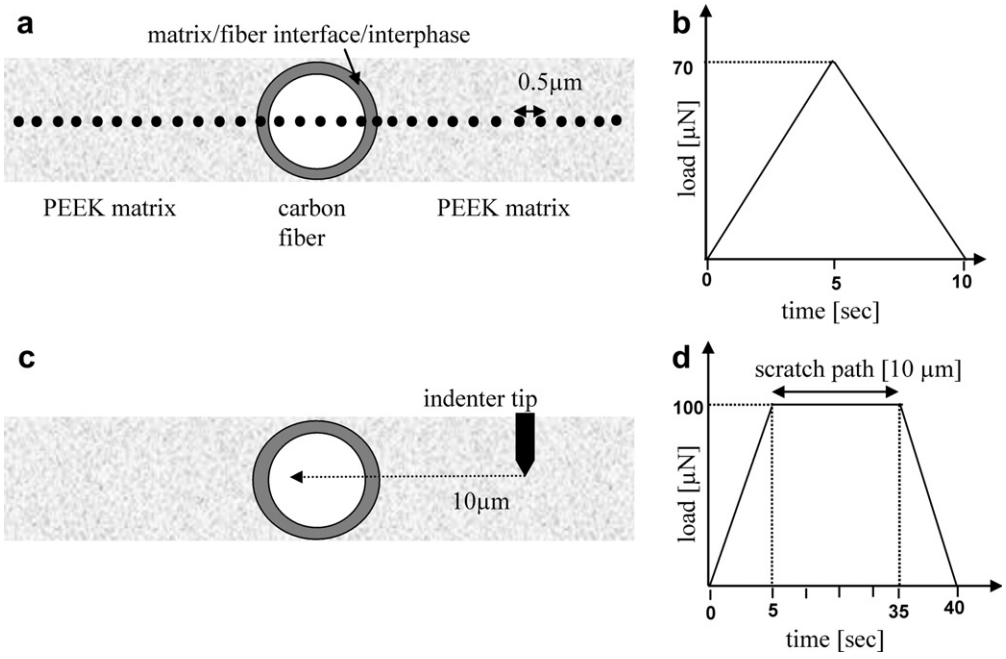

Fig. 2. Scheme of the nanoindentation test protocol displaying: (a) a nanoindentation pattern of 1×50 indents with each of the successive indents separated by 0.5 μm and (b) the triangular loading–unloading function with 70 μN as peak load and 5 s each for both loading and unloading without any holding time. The nanoscratch test protocol displays (c) the scratch path covering a part of the carbon fiber surface and of the PEEK matrix and (d) the scratch test loading–unloading function with 100 μN maintained as the peak load during a scratch path of 10 μm.

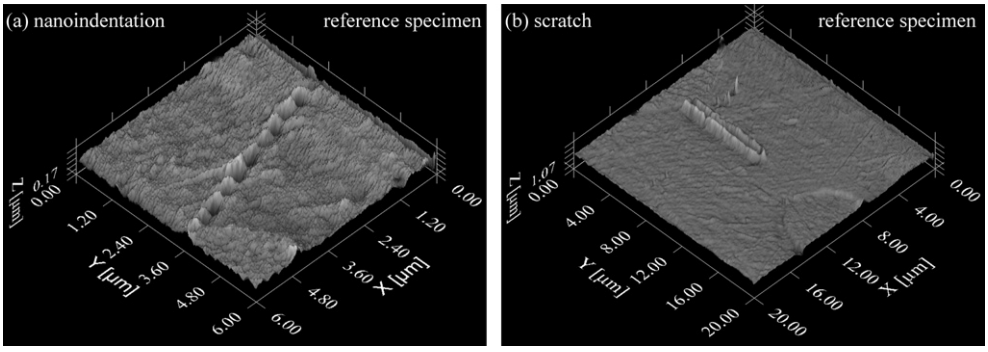

Fig. 3. Surface topography of the reference specimen (no sterilization treatment) of the carbon fiber-reinforced PEEK composite: (a) after nanoindentation testing, showing a line of indents in the matrix, and (b) after nanoscratch testing, showing the scratch path in the matrix.

displacement data, the indenter contact area function was derived from indentation tests conducted previously on a quartz standard sample.

2.4.2. Nanoscratch test protocol

A nanoscratch test is performed by moving the indenter tip while it is in contact with the sample surface, as outlined in detail above. The used Berkovich indenter was oriented with one of its sharp edges pointing in the scratch direction. Thereby, the indenter tip scratches the sample surface more evenly. The applied peak load of 100 μN was achieved within 5 s, and after conducting a scratch of 10 μm at a speed of around 0.33 μm s^{-1}, it was removed again during 5 s, as shown in Fig. 2d. The scratch length at peak load was limited to about 10 μm, starting from the matrix and ending at the fiber surface. Hence, it was not possible to investigate the matrix/fiber interphase regions on both side of a single fiber in the course of one scratch experiment. The experiments were repeated several times for each specimen at different positions of the matrix/fiber arrangement.

3. Results

3.1. Nanoindentation results

The representative load–displacement curves obtained from the indentation tests performed at maximum peak load of 70 μN for the reference specimen are illustrated in Fig. 4. Based on the indentation depth values, the different regions are schematically indicated on top of the curves in Fig. 4. The indentation depth values range from 20 nm for the fiber region to 85 nm for the bulk matrix region. The carbon fibers exhibit almost identical loading–unloading paths whereas the matrix region showed significantly different paths through the formation of a hysteresis loop. This hysteresis behavior is explained by the viscoelastic recovery due to the relaxation of elastic strains with the matrix. The few curves at intermediate indentation depth represent the transition region formed by the matrix around the carbon fibers estimated as the interphase. The properties of the interphase region also seem to vary, as indicated by the scatter of the curves in this region. A similar pattern of the load–displacement curves was observed for both the steam-treated and the gamma-irradiated test specimens, but with slightly different indentation depth values in the different regions (fiber, interphase zone, bulk matrix).

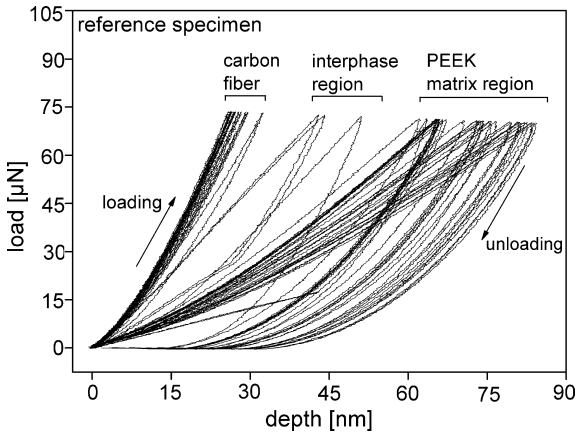

Fig. 4. Some representative load–displacement curves displaying the micromechanical behavior of the reference (no sterilization treatment) carbon fiber-reinforced PEEK composite during nanoindentation performed at a peak load of 70 μN.

For further quantitative analysis of the micromechanical properties, the hardness and the reduced elastic modulus values as calculated by the Oliver and Pharr method [31] are plotted against the indentation path (Fig. 5). The micromechanical behavior of the reference specimen is shown in Fig. 5a. The different regions are defined according to the values of the reduced elastic modulus, which range from 4 to 12 Gpa, and the values of the hardness, which range from 0.1 to 0.3 GPa. The sites with low hardness and low modulus indicate the matrix region whereas the higher values reveal the position of the fiber surface. There is 20–30% fluctuation in the values at the fiber regions for all the specimens (Fig. 5a–c), which is due to the roughness of the fiber surface. The final polishing step was performed using a paste consisting of 50-nm-wide abrasive particles which generated a level of roughness of 10–15 nm and formed a ridged surface, i.e. formation of "peaks and valleys". The influence of such nanoscale roughness is more pronounced when the indentation depth is of the same order, which is in the fiber regions in the present study. The location of the interface, i.e. of the actual fiber edge, is identified by the sudden increase in the hardness and the reduced elastic modulus. It is referred to as the *estimated interface* in Fig. 5a. A similar analysis was performed for the steam-treated and gamma-irradiated specimens, as displayed in Fig. 5b and c, respectively.

The zones identified as interphase regions show different values in the mechanical properties, namely slightly higher ones than the matrix but much lower ones than the fibers. The interphase width for the reference specimen has an extension of about 0.7 μm, which is similar to the width of the interphase zone observed for both the steam-treated and gamma-irradiated specimens. The steam-treated specimen shows the interesting trend of an increased value of the reduced elastic modulus near the estimated interface, indicating a modification in the properties of the PEEK matrix in this region.

3.2. Nanoscratch results

The nanoscratch tests provide a qualitative measure for the friction properties at the surface. The method which was described in detail by Hodzic et al. [24] is adopted in the present study for the analysis of scratch paths. The test proceeds by recording the depth profile and the coefficient of friction while the indenter tip is scratching over the surface. Eighteen different scratch cycles were conducted in order to achieve meaningful statistics, as illustrated schematically in Fig. 2c and as documented in the surface

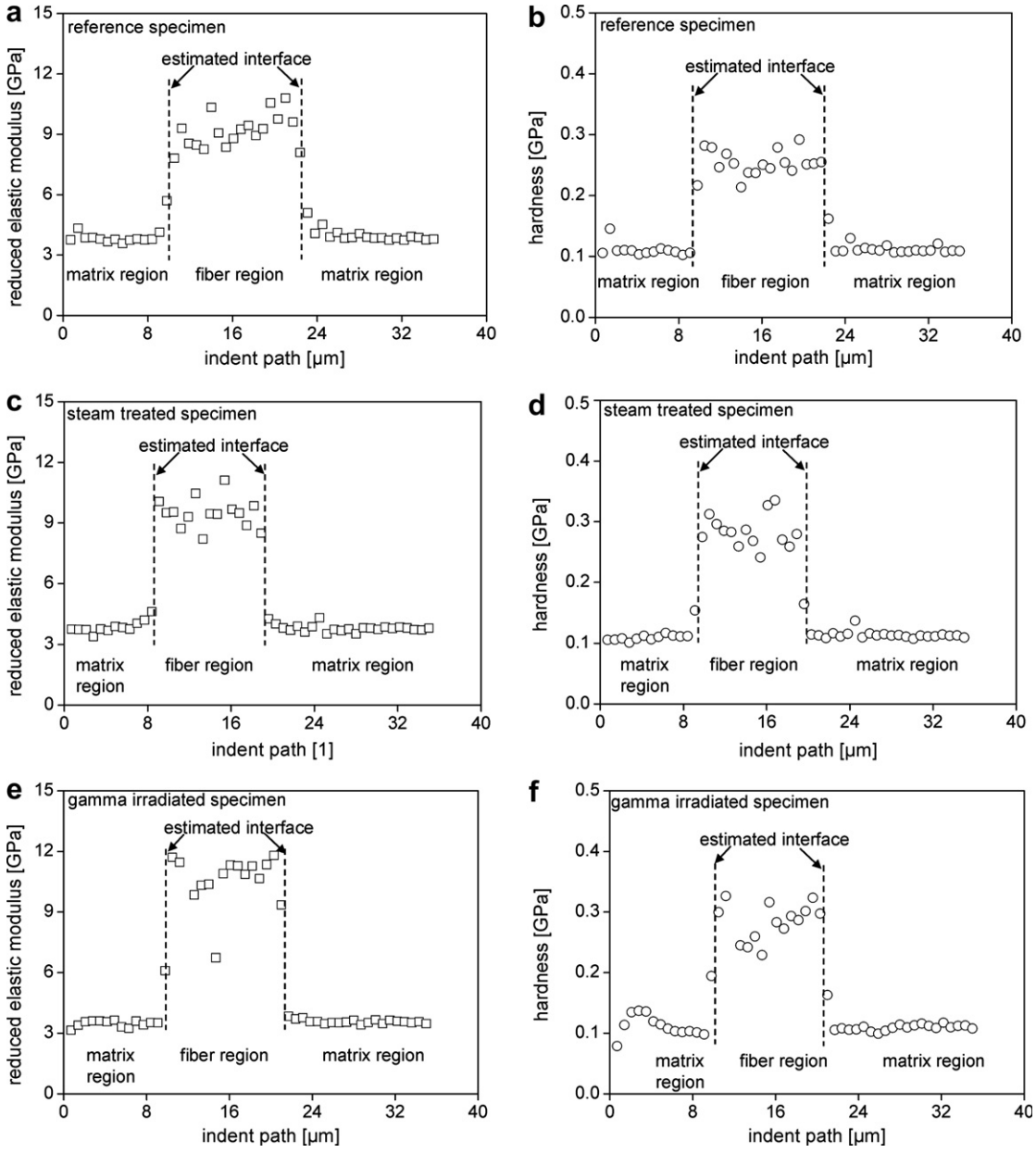

Fig. 5. Indentation response showing the reduced elastic modulus and the hardness of the matrix/fiber arrangement for the reference specimen (a and b); the steam-treated specimen (c and d); and the gamma-irradiated specimen (e and f). The dotted lines marked as "estimated interface" indicate the transition between the matrix and the fiber regions.

topography in Fig. 3b. The data obtained for the different scratch paths were very similar, so for the sake of clarity only one representative scratch path for each test specimen will be discussed in detail in this study.

The penetration depth is determined by the contact length between the leading edge of the indenter tip and the material indented. It is influenced by various factors, such as the hardness, the modulus and the wear resistance of the material being scratched. In Fig. 6, following the scratch direction from the matrix towards a fiber surface, all the curves show a deviation from their normal path, indicating a change in the properties of the scratched material. The tangents of the slopes of the deviations in the friction coefficient in the vicinity of such interfaces were used to identify the micromechanical transition regions. Based on the intersection points between two tangents (constant level outside of the transition zone, slope within the transition zone, see Fig. 6), different regions were identified on the scratch path, revealing the micromechanical characteristics of the material in the vicinity of the fibers.

Fig. 6a shows the scratch response of the reference specimen which was not treated by a sterilization process. Following the scratch direction in Fig. 6a, a high indentation depth can be observed outside of the transition zone, as expected, indicating the softer characteristics of the matrix. This observation is in good agreement with the high coefficient of friction in the same region. At this stage the indenter is still moving entirely within the matrix region. After

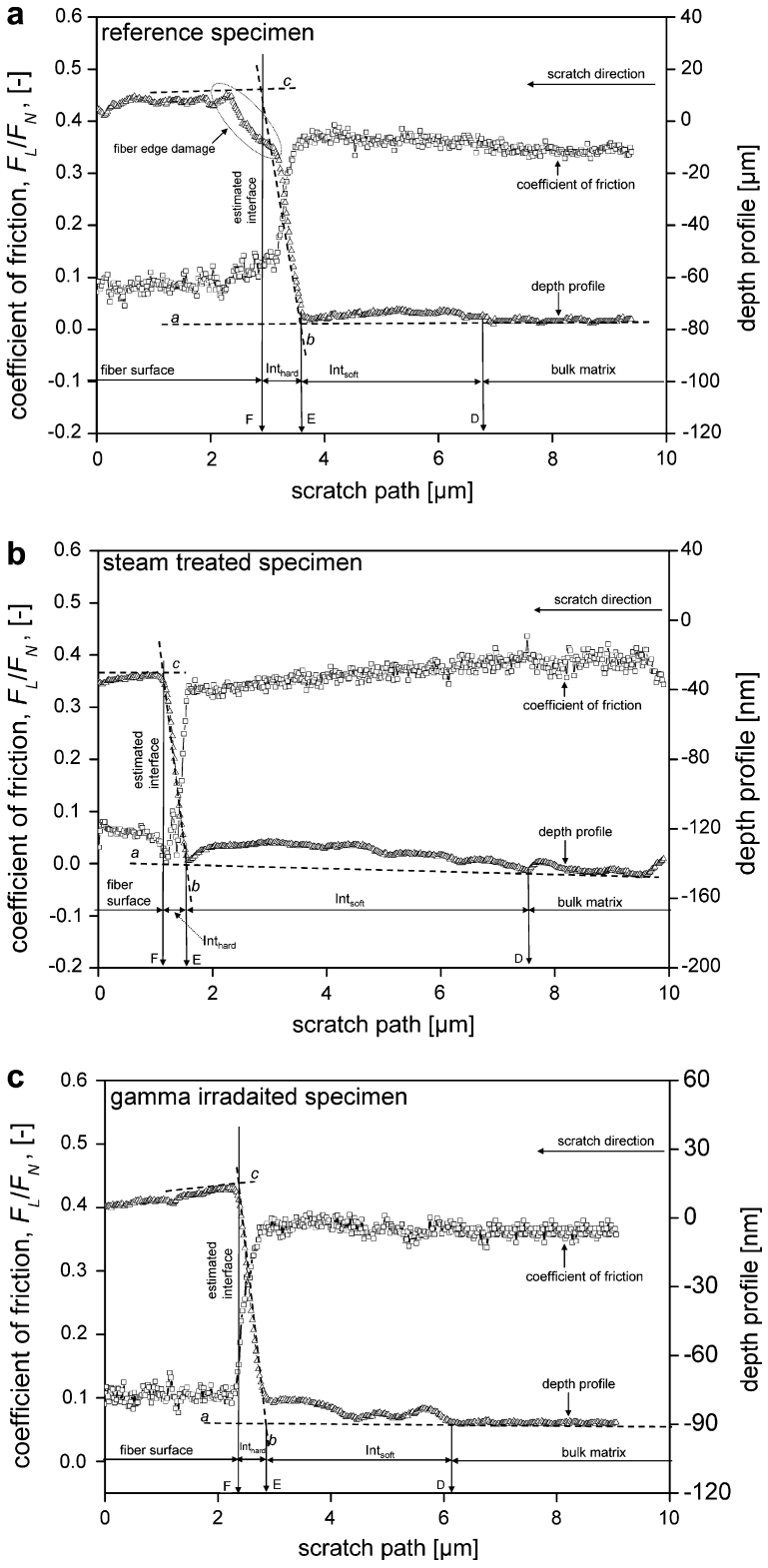

Fig. 6. Scratch profile analysis [24] of the matrix/fiber arrangement in the PEEK/CF composite for (a) the untreated reference specimen, (b) the steam-treated specimen and (c) the gamma-irradiated specimen with a constant applied load of 100 μN. The dotted tangent lines *a*, *b* and *c* mark the changes in the slopes of the depth profile in the different regions. The points D, E and F mark different regions along the scratch path. These are (i) the fiber surface (region left of point F); (ii) the hard interphase region, formed by the chemical coating of the carbon fiber surface and the matrix, Int_{hard} (between points F and E); (iii) the soft interphase region, formed by the modified morphology of the matrix, Int_{soft} (between points E and D); and (iv) the bulk matrix (to the right of point D). The coefficient of friction, μ, is determined from the ratio of the lateral force, F_L (tangential force), and the normal force, F_N, with a constant applied load of 100 μN.

this there is a departure from the normal depth profile, which indicates a change in the material properties. This point is marked as D on the abscissa along the scratch path. Tangent *a* was drawn to indicate the change in the slope of the depth profile. As the indenter moves further towards the actual interface between fiber and matrix, the gradual decrease in the penetration depth is followed by a very steep decrease in the penetration depth with a very sharp change of the slope, indicated by tangent *b*. The gradual decrease in the penetration depth indicates a gradient in the micromechanical properties whereas the large decrease and the sharp change in slope suggests that the indenter came into contact with a very hard surface.

Based on the corresponding data for the coefficient of friction, the edge of the fiber surface may be assumed to be the reason for such a sharp transition in the slope of the depth profile. Hence this position was marked as the estimated interface between the fiber and the matrix. The tangent *c* indicates the slope of the depth profile in the fiber region. All tangents were extrapolated and the intersection point of tangents *a* and *b* was marked as point E on the scratch path, while the intersection point of tangents *b* and *c* was marked as point F, which is referred to as the estimated interface. Based on the analysis described above, points D, E and F on the scratch path provide very useful information about the positions of the micromechanically relevant zones in the composite material relative to the local microstructure. On the right side of point D the indenter was moved entirely in the bulk matrix, while between points D and F it still moved in the matrix but showed a different behavior. The continuous change of the slope between points D and F further suggests a transition of properties in this zone. The total thickness of this transition zone (W_{trans}) is referred to as the interphase region according to the definition given above. Point E divides this zone into regions Int_{hard} and Int_{soft}. The region Int_{hard} (hard interphase) is formed by the chemical coating of the fiber surface and the matrix very close to it (zone between points E and F). The region Int_{soft} (soft interphase) is formed by the matrix zone between points D and E, which is abutting to the bulk matrix [32,33].

The response of the steam-treated and the gamma-irradiated specimens is shown in Fig. 6b and c, respectively. Although the various curves are basically similar, the influence of the sterilization treatment can be best observed in terms of the change in the slopes of the depth profiles. Based on the different regions marked on the scratch path, the estimated thickness of the interphase region for the reference specimen is ~3 μm. For the gamma-irradiated specimen it showed a slight change, increasing to ~3.8 μm, whereas for the steam-treated sample it amounted to ~5.3 μm (Fig. 7).

4. Discussion

4.1. Hardness

The average values of the elastic modulus (~3.5 GPa) and hardness (~0.12 GPa) of the bulk matrix region for the sterilized specimens are very similar to the respective values observed for the reference specimen (Fig. 5). This fact indicates the structural stability of the material at the nanoscale under the employed sterilization methods. Consequently, similar observations may be expected for the overall mechanical behavior of the material. It is difficult to estimate the width of the interphase region by nanoindentation experiments based on the hardness values of the region. However, overall trends of the hardness results are in accordance with previous studies, i.e. they display a significant influence of the hard fiber surfaces on the morphological properties of semicrystalline polymers when they are in contact with a solid surface while solidifying [1–3]. This is explained by the cumulative influence of the enhanced rate of nucleation during the crystallization process and the parallel alignment of polymer chains along the solid surfaces provided by the fibers embedded. The localized enhancement in the rate of nucleation reduces the final size of the crystalline spherulites in the vicinity of the fiber

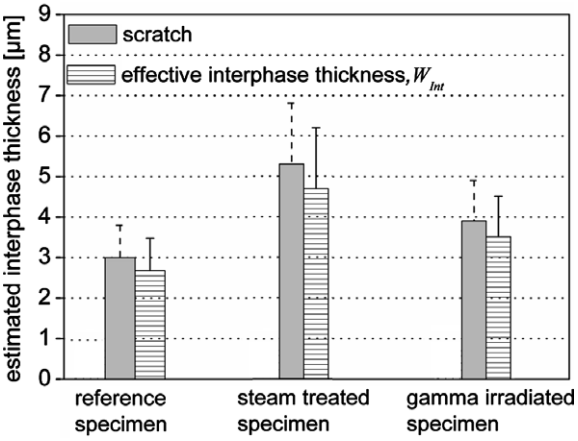

Fig. 7. Estimated thickness of the interphase region determined by the nanoscratch testing. The comparison with the effective interphase thickness, W_{Int}, is also shown.

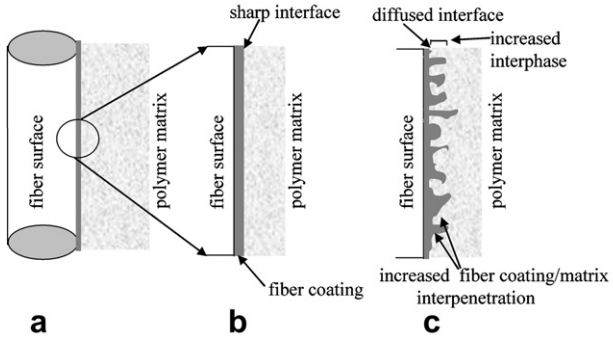

Fig. 8. Schematic illustration of: (a) a fiber–matrix arrangement, (b) a fiber coating and a sharp interface at the fiber–matrix interface, and (c) a diffused interface between the matrix and the fiber coating causing an increase in the interphase thickness [25,26].

surfaces, which in turn modifies the morphological properties of the matrix in that region. This modified morphology influences both the adhesion between the carbon fibers and the PEEK matrix as well as the micromechanical properties [20–23]. The presence of fibers can also impose restrictions on the normal plastic-flow deformation mechanism of the matrix, hence inducing an artificial increase in the hardness values within the proximity of the fiber surface.

4.2. Interphase

The morphologically modified matrix with additional effects of chemical bonding and inter-diffusion at the interface forms the interphase. The thickness of this interphase region depends on many factors, such as the properties of the matrix, the fiber surface, the rate of solidification, the fiber content and the fiber surface coating (also referred to as sizing) [20–23]. The change in the width of the interphase region inferred from the scratch tests suggests that the sterilization process probably further induces morphological changes in the state of the matrix (Fig. 8). As explained by Hodzoic [24,25], the formation of the interphase region between phenolic resin and glass fibers is a cumulative effect of the inter-diffusion process and the chemical bonding between the fiber surface and the polymer matrix, at both the interface and the interphase regions.

Elevated temperatures and enhanced pressure in the presence of moisture during the steam sterilization process probably promotes further chemical bonding and higher inter-diffusion rates. These effects would entail an increase in the size of the interphase. Such an increased inter-diffusion zone can also generate a transition in the interphase region, with a harder zone in the area next to the fiber and a softer one more remote from it. Our observations in that context are in accordance with similar behavior observed before in a silane-treated glass fiber–polyester interphase system studied by Hodzic et al. [25]. Fig. 8 gives a schematic illustration of the modification in the polymer matrix properties surrounding a chemically coated fiber. Such modifications are the result of interpenetration of the chemical and the matrix under the influence of sterilization processes or under other environmental exposure [25,26]. The results of gamma irradiation are consistent with previous studies of UV irradiation environmental ageing conducted by Nowicki et al. [27] performed on thin films of polyvinyl chloride, polyethylene oxide and polyacrylic acid.

4.3. Factors influencing the results

Although the results of the indentation and scratch tests are partially in agreement, both separately provide a detailed insight into the three main micromechanically relevant zones in the composite (fiber, interphase zone, bulk matrix). Some experimental factors shall be discussed in the following which may be responsible for a certain scatter in the data and also for some of the deviations observed between the two types of tests. Starting from the sample preparation to performing the final experiments, if one considers all the different factors involved during the tests, such as roughness of the surface, microstructure inhomogeneity, the exact location of the indentation and scratch paths, the final results may vary quantitatively. The following sections address some of these aspects in more detail.

4.3.1. Surface roughness

The two important goals when polishing the specimens prior to the mechanical tests are first, to introduce very little interfacial stress, which may cause premature interfacial cracking and artificial surface hardening effects; and second, to produce a very flat surface with negligible relief effects between fiber and matrix. However, it is conceivable that during such a procedure a fiber becomes cracked or crushed if it is raised above the surface. Such effects were indeed observed, as documented by the optical micrograph shown in Fig. 1. The final surface polishing was conducted using a 50 nm wet diamond suspension, which leads to a roughness of the sample surface of around 10–15 nm, as indicated by surface topography analysis (Fig. 3). As shown in earlier work [24], such tiny roughness values can produce a scatter of 10–15% in the mechanical data obtained from nanoindentation testing, which is in accordance with our results. Desaeger et al. [34] showed a 40% difference in the debonding loads by simply changing the polishing procedure for the carbon fibers and the different thermoplastic and thermoset polymer matrices such as epoxy, polypropylene and polyamide.

4.3.2. Microstructure inhomogeneity

The random fiber orientation also plays an important role in this study since this effect renders the microstructure inhomogeneous. For instance, in the indentation tests, the scatter in the hardness values obtained in the matrix regions far away from the fiber surface inspected may well be due to the presence of other fibers underneath the matrix surface. Due to the thickness of the material and the stochastic spacing between the randomly oriented fibers, overlapping of the interphase regions is another issue to consider before aiming at drawing quantitative conclusions. Therefore, in the scratch tests the test regions (fiber/matrix arrangement) were chosen very carefully to avoid any constraint influences caused by the presence of other surrounding fibers, but the effect cannot be completely ruled out.

4.3.3. Indenter geometry

The thickness of the transition zone which is estimated as the interphase region between the carbon fiber and the PEEK matrix not only reflects the actual interphase thickness, but also includes the region created by the lateral resolution of the indenter geometry. This lateral resolution, therefore, must be defined as the indenter width, W_{Ind}. Hodzic et al. [24] described such influences in detail,

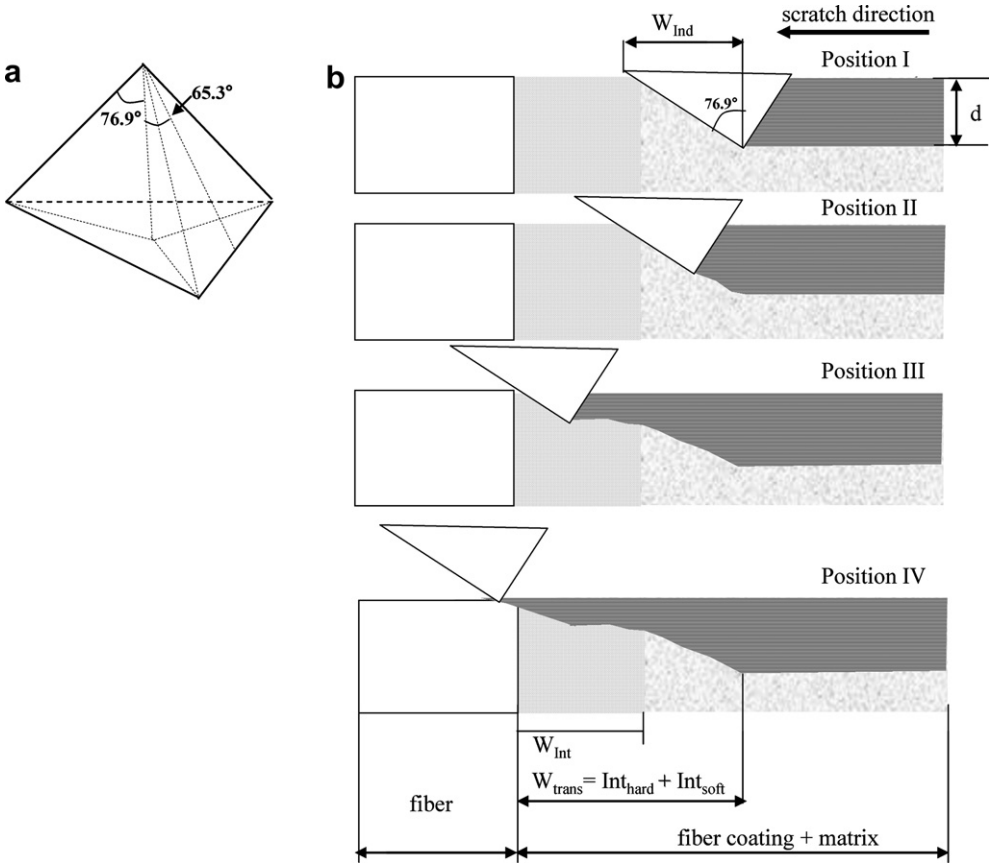

Fig. 9. (a) Geometry of the Berkovich indenter tip. (b) Schematic illustration of depth profiles at different positions during the progression of a nanoscratch test. W_{Ind} is the indenter width, d is the scratch penetration depth, W_{Int} is the effective interphase thickness and W_{trans} is the total thickness of the transition region [24].

considering different cases for the interphase thickness. However, in the present study only the relevant case where the interphase thickness exceeds the indenter width, as indicated by the larger total thickness of the transition zone, W_{trans}, is discussed. Fig. 9 shows a schematic illustration of the geometry of a Berkovich indenter as used in this study and the position of the indenter at various stages during the progression of a scratch test. At position I, the indenter tip is moving in the bulk matrix while the leading edge of the indenter touches the edge of the interphase for the first time. At position II, the interaction between the leading edge of the indenter and the interphase region causes a gradual decrease in the depth profile though the indenter tip is still moving in the matrix region. At position III, a similar interaction is expected between the leading edge of the indenter and the fiber edge, but with a much higher slope because of the harder edge of the fiber. This can cause slight wearing of the fiber edge, generating rounding-off as a consistent feature in the depth and the coefficient profiles at the estimated interface, as seen in Fig. 6. The hard edge of the fiber surface may undergo damage, as indicated in Fig. 6a, and cause slipping of the leading edge of the indenter rather than scratching over its surface. Such effects, which are hard to avoid owing to the geometry of the indenter, may cause inconsistent results. At position IV, once the indenter tip is completely on the fiber surface, both the depth profile and the coefficient profile show reduced values.

Because of the indenter geometry and the penetration depth, one can separate the effective interphase thickness, W_{Int}, from the total thickness of the transition zone ($Int_{hard} + Int_{soft}$), W_{trans}, by using the following equation:

$$W_{Int} = W_{trans} - d \tan \theta \quad (7)$$

where d is the scratch penetration depth and θ is the scratch tip angle = 76.9° (Fig. 9).

The difference between the total thickness of the interphase, also referred to as the transition zone (the distance between points D and F in Fig. 6), and the effective thickness of the interphase is not very significant (Fig. 7). This observation suggests that there is a minimal influence of the interaction between the indenter geometry and the interphase edge. This is because the soft part of the interphase region, Int_{soft}, is unable to resist the movement of the leading edge of the indenter when compared with the stiffer response of the hard fiber edge.

5. Conclusions

The complementary experimental approach of using nanoindentation and nanoscratch tests proved very successful in investigating the influence of two types of

sterilization processes on the interphase properties of a carbon fiber-reinforced PEEK composite. The nanoindentation tests were used to determine the properties of the different micromechanically relevant zones, such as the bulk PEEK matrix, the interphase region and the carbon fibers present in the material. The nanoscratch tests revealed more details about the physical and micromechanical changes in the interphase region being continuously in contact with the surface. The latter method, hence, appeared to be a more sensitive and reliable technique in detecting the interphase properties. The continuity in data acquisition obtained from the nanoscratch tests was crucial for the analysis of the gradients in the micromechanical properties within the PEEK matrix. The data reveal that the bulk polymer is largely unaffected in terms of the measured parameters by sterilization and only a slight modification in the properties of the PEEK matrix occurs at the interphase. This applies in particular to the steam sterilization process.

References

[1] Lustiger A, Uralil FS, Newaz GM. Processing and structural optimization of PEEK composites. Polym Compos 1990;11:65–75.

[2] Saiello S, Kenny J, Nicolais L. Interface morphology of carbon fiber/PEEK composites. J Mater Sci 1990;25:3493–6.

[3] Zhang M, Xu J, Zhang Z, Zeng H, Xiong X. Effect of transcrystallinity on tensile behavior of discontinuous carbon fiber-reinforced semicrystalline thermoplastic composites. Polymer 1996;37:5151–8.

[4] Ray BC. Temperature effect during humid ageing on interfaces of glass and carbon fibers reinforced epoxy composites. J Colloid Interface Sci 2006;298:111–7.

[5] Kaelble DH, Dynes PJ, Maus L. Hydrothermal aging of composite-materials. 1. Aspects. J Adhesion 1976;8:121–44.

[6] Marom G, Broutman LJ. Moisture in epoxy resin composites. J Adhesion 1981;2:153–64.

[7] Mijovic M, Lin K-F. The effects of hygrothermal fatigue on physical mechanical properties and morphology on neat epoxy-resin and graphite composite. J Appl Poly Sci 1985;30:2527–49.

[8] Barraza HJ, Aktas L, Hamidi YK, Long Jr J, O'Rear EA, Altan MC. Moisture absorption and wet-adhesion properties of resin transfer molded (RTM) composites containing elastomer-coated glass fibers. J Adhesive Sci Technol 2003;17:217–42.

[9] Zheng Q, Morgan RJ. Synergistic thermal—moisture damage mechanisms of epoxy and their carbon-fiber composites. J Compos Mater 1993;27:1465–78.

[10] Lee MC, Peppas NA. Models of moisture transport and moisture-induced stresses in epoxy composites. J Compos Mater 1993;27:1146–71.

[11] Vaddadi P, Nakamura T, Singh RP. Transient hygrothermal stresses fiber reinforced composites: a heterogeneous characterization approach. Compos A: Appl Sci Manuf 2003;34:719–30.

[12] Mensitieri G, Apicella A, Kenny JM, Nicolais L. Water sorption kinetics in poly(aryl ether ether ketone). J Appl Poly Sci 1989;37:381–92.

[13] Wolf CJ, Fu H. Stress enhanced sorption of water in poly(ary1 ether ether ketone) [PEEK]. J Poly Sci, Part B: Poly Phys 2003;33:331–2.

[14] Lee SM, Choi SW, Nho YC, Song HH. Modification of microstructures and physical properties of ultra high molecular weight polyethylene by electron beam irradiation. J Poly Sci, Part B: Poly Phys 2005;43:3019–29.

[15] Premnath V, Bellare A, Merrill EW, Jasty M, Harris WH. Molecular rearrangements in ultra high molecular weight polyethylene after irradiation and long-term storage in air. Polymer 1999;40:2215–29.

[16] Shinde A, Salovey R. Irradiation of ultrahigh-molecular-weight polyethylene. J Polym Sci Polym Phys Ed 1985;23:1681–9.

[17] Sasuga T, Seguchi T, Sakai H, Nakakura T, Masutani M. Electron-beam irradiation effects on mechanical properties of PEEK/CF composite. J Mater Sci 1989;24:1570–4.

[18] Vaughan AS, Suttor SJ. On radiation effects in oriented poly(ether-ether ketone). Polymer 1995;36:1549–54.

[19] Vaughan AS, Stevens GC. Irradiation and the glass transition in PEEK. Polymer 2001;42:8891–5.

[20] Gao SL, Kim JK. Cooling rate influences in carbon fiber/PEEK composites. Part I: crystallinity and interface adhesion. Composites: Part A 2000;31:517–30.

[21] Gao SL, Kim JK. Cooling rate influences in carbon fiber/PEEK composites. Part II: interlaminar fracture toughness. Composites: Part A 2001;32:763–74.

[22] Gao SL, Kim JK. Cooling rate influences in carbon fiber/PEEK composites. Part III: impact damage performance. Composites: Part A 2001;32:775–85.

[23] Gao SL, Kim JK. Correlation among crystalline morphology of PEEK, interface bond strength, and in-plane mechanical properties of carbon/PEEK composites. J Appl Polym Sci 2002;84:1155–67.

[24] Hodzic A, Stachurski ZH, Kim JK. Nanoindentation of polymer–glass interfaces. Part I: Experimental and mechanical analysis. Polymer 2000;41:6895–905.

[25] Hodzic A, Kim JK, Stachurski ZH. Nanoindentation and nanoscratch of polymer/glass interfaces. Part II: Model of interphases in water aged composite materials. Polymer 2001;42:5701–10.

[26] Gregory JR, Spearing SM. Nanoindentation of neat and in-situ polymers in polymer–matrix composites. Compos Sci Technol 2005;65:595–607.

[27] Nowicki M, Richter A, Wolf B, Kaczmarek H. Nanoscale mechanical properties of polymers irradiated by UV. Polymer 2003;44:6599–606.

[28] Gao SL, Mäder E. Characterization of interphase nanoscale property variation in glass fiber-reinforced polypropylene and epoxy resin composites. Composites: Part A 2002;33:559–76.

[29] Tai NH, Yip MC, Tseng CM. Influences of thermal cycling and low-energy impact on the fatigue behavior of carbon/PEEK laminates. Composites: Part B 1999;30:849–65.

[30] The national and international quality management system standards. EN ISO 9001:2000 and ISO 13485:2003.

[31] Oliver WC, Pharr GM. An improved technique for determining the hardness and elastic modulus using the load and displacement sensing indentation experiments. J Mater Res 1992;7:1564–83.

[32] Mai K, Mäder E, Mühle M. Interphase characterization in composites with new non-destructive methods. Composites A 1998;29:1111–9.

[33] VanLandingham MR, McKnight SH, Palmese GR, Bogetti TA, Eduljee RF, Gillespie Jr JW. Characterization of interphase regions using atmic force microscopy. J Adhesion 1997;64:31–59.

[34] Desaeger M, Verpoest I. On the use of the micro-indentation test technique to measure the interfacial shear strength on fiber-reinforced polymer composites. Compos Sci Technol 1993;48:215–26.